HYDROLOGICAL PROCESSES
Hydrol. Process. **15**, 2917–2930 (2001)
DOI: 10.1002/hyp.382

Simulating overland flow following wildfire: mapping vulnerability to landscape disturbance

Peter C. Beeson,[1] Scott N. Martens[2] and David D. Breshears[1]*

[1] *Environmental Dynamics and Spatial Analysis, Los Alamos National Laboratory, Mail Stop J495, Los Alamos, NM 87545, USA*
[2] *Department of Land, Air, and Water Resources, University of California Davis, Davis, CA 95616, USA*

Abstract:

The probability of landscape-scale disturbances such as fire are expected to increase in the future due to anticipated climate changes and past land management practices. These disturbances can produce dramatic changes in hydrologic responses (e.g. overland flow) that can pose risks to human life, infrastructure, and the environment. Assessing these risks and associated remediation strategies requires spatially explicit evaluation of upland hydrology. However, most current evaluation methods focus on a specified location within a watershed, precluding estimation of spatially distributed, upland, hydrological response; and those that do consider spatial variability usually do not account for redistribution of overland flow among adjacent subunits. Here we highlight the use of a spatially distributed model for assessing spatial changes in upland hydrologic response following landscape-scale disturbance. Using a distributed model called SPLASH (Simulator for Processes of Landscapes: Surface/Subsurface Hydrology), we simulated pre- and post-fire scenarios based on the Cerro Grande fire (Los Alamos, NM, USA; May 2000) over 17 300 ha (resolution of 30 m × 30 m) for 2 year and 100 year design storms. For the 2 year storm, maximum overland flow rates for burned cells in the post-fire scenario greatly exceeded those for pre-fire conditions (modes: pre-fire, $3{\cdot}25 \times 10^{-10}$ m^3 s^{-1}; post-fire, $7{\cdot}0 \times 10^{-10}$ m^3 s^{-1}). For the 100 year storm, maximum overland flow was much greater than for the 2 year storm (modal pre-fire: $31{\cdot}8 \times 10^{-10}$ m^3 s^{-1}), with the difference between pre- and post-fire simulations being less dramatic (modal post-fire: $48{\cdot}6 \times 10^{-10}$ m^3 s^{-1}). Mapped differences between pre- and post-fire provide a means for prioritizing upland areas for remediation using an approach that accounts not only for topography, soils, and plant cover, but also for the redistribution of overland flow. More generally, our results highlight the potential utility of spatially distributed models to focus and prioritize rehabilitation efforts for future assessments of risk following landscape-scale disturbance. Copyright © 2001 John Wiley & Sons, Ltd.

KEY WORDS hydrologic model; runoff; risk assessment; semiarid

INTRODUCTION

Hydrological responses such as overland flow are intimately interrelated with landscape surface characteristics. Moreover, hydrological response can change greatly when landscape surface characteristics are altered through environmental disturbances, such as drought or fire. For example, drought-induced plant mortality can occur at the landscape-scale, as happened in the southwestern USA during the 1950s (Herbel *et al*., 1972; Regensberg, 1996; Allen and Breshears, 1998). These changes in surface characteristics can apparently trigger large increases in rates of runoff and erosion (Wilcox *et al*., 1996, 1997; Davenport *et al*., 1998). Of particular note are the large increases in overland flow that can follow wildfire and the potential for high sedimentation rates, debris flows, and other channel impacts (e.g. Morris and Moses, 1987; Meyer and Wells, 1997; Cannon *et al*., 1998; Wilson, 1999; Cannon and Reneau, 2000). The impacts of increased overland flow and sediment yield are a result of net increases in flow energy. The amount of energy can be increased following fire not

* Correspondence to: D. D. Breshears, Environmental Dynamics and Spatial Analysis, Los Alamos National Laboratory, Mail Stop J495, Los Alamos, NM 87545, USA. E-mail: daveb@lanl.gov

Received 1 April 2001
Accepted 9 July 2001

only because of reductions in vegetation cover and surface roughness, but also due to changed soil properties that can increase water repellency (or hydrophobicity) (DeBano, 2000).

The importance of post-fire overland flow is likely to increase in the future because changes in climate and past land use practices lead to increased probability of landscape-scale wildfires. Climate can drive fire frequencies on a subcontinental scale, as found for El Niño/Southern Oscillation (ENSO) in the southwestern USA (Swetnam and Betancourt, 1990). Fires were frequent and probably of low intensity prior to the late 1800s (Allen *et al*., 1998; Swetnam and Betancourt, 1998; Swetnam *et al*., 1999). In some areas, subsequent fire suppression led to increased tree density of more than an order of magnitude. (Covington *et al*., 1994; Mast *et al*., 1999; Moore *et al*., 1999). Consequently, large portions of the western USA are at risk from forest fires. This risk is exacerbated by changes in climate (Lenihan *et al*., 1998), which have been documented for the latter part of the 20th century and are projected to increase under many global climate change scenarios (Easterling *et al*., 2000). In particular, two types of extreme climatic events are likely to become more frequent and intense—droughts, which would increase the probability of wildfire, and large episodic storms, which would increase post-fire runoff and erosion. Therefore, assessing hydrologic response to landscape-scale disturbance (e.g. fire and drought) is increasingly important.

In the wake of post-fire changes in landscape characteristics, rapid assessments are conducted to determine the best strategies for remediation of upland areas, as highlighted by reports from Burned Area Emergency Rehabilitation (BAER) teams. Post-fire hydrological responses can pose immediate and serious threats to human life, infrastructure, and environmental systems. Addressing these issues and establishing remediation priorities requires focusing on strategies for upland areas, such as felling logs perpendicular to the slope, breaking up areas of hydrophobic soils, and planting seeds and seedlings (Robichaud *et al*., 2000). However, as time and funding are critical constraints for determining post-fire remediation strategies, it is essential to identify the most important upland areas for remediation. Most post-fire remediation efforts for landscape-scale fires do not utilize spatially distributed inputs to produce fully distributed predictive output. Rather, most current methods focus on a few locations—usually those deemed critical on the basis of risks to life and infrastructure—and do not allow for development of a spatially distributed map of post-fire vulnerability (e.g. McLin *et al*., 2001). Even those methods that are spatially distributed usually do not account for cell-to-cell routing of water associated with topographic variations in the landscape to arrive at their results (e.g. Wilson *et al*., 2001). The role of redistribution of runoff from smaller spatial units up to catchment/watershed scales varies among sites and is critically important (Prosser and Williams, 1998). The spatial redistribution of water depends on the properties of both the hydrological source and sink units and their hydrological connectivity (e.g. Dietrich *et al*., 1993; Seyfried and Wilcox, 1995; Davenport *et al*., 1998; Herron and Wilson, 2001). Hence, the redistribution of water among cells is important to evaluate; yet this has rarely been considered in studies to date.

Here we highlight how a spatially distributed model can be used to assess landscape-scale changes in hydrologic response following disturbance. This approach can be used to map upland areas of highest vulnerability to post-fire runoff and to help prioritize remediation efforts. Using a distributed ecohydrological model called SPLASH (Simulator for Processes of Landscapes: Surface/Subsurface Hydrology), we simulated pre- and post-fire scenarios based on the Cerro Grande fire, which burned nearly 17 300 ha near Los Alamos, New Mexico, USA, during May 2000. We evaluated design storms of two return probabilities: 2 years and 100 years. Our simulations were high resolution (30 m × 30 m cell size) and extensive, yielding calculations for more than 670 000 cells. The mapped results from these types of high-resolution simulations provide a means for better addressing post-fire assessments in the future.

SITE DESCRIPTION

The Pajarito Plateau

The Pajarito Plateau flanks the east side of the Jemez Mountains in northern New Mexico. The plateau comprises an elevational gradient ranging from near 1600 m towards the east to more than 3200 m towards

the west. There are pronounced canyon/mesa topographic dissections running east to west. The climate is monsoonal, with two major periods of precipitation: winter snow and summer thunderstorms (Bowen, 1990). Precipitation is related to elevation, with mean annual precipitation of ~400 mm near 2100 m elevation. The parent material for the vast majority of soils is Bandelier Tuff of volcanic origin (Nyhan *et al*., 1978). Soils descriptions are provided in Nyhan *et al*. (1978), Davenport *et al*. (1996), USDA (1994), and Benally (1991). The vegetation patterns are related to elevation and associated changes in plant-available water (Barnes, 1986; Allen, 1989; Padien and Lajtha, 1992; Martens *et al*., 2001). Lower elevation mesa tops are dominated by juniper savanna transitioning into piñon–juniper woodlands (*Pinus edulis* and *Juniperus monosperma*), mid elevations are dominated by ponderosa pine forest (*Pinus ponderosa*), and upper elevations are mixed confer forest.

Hydrological studies

Several hydrologic aspects of the Pajarito Plateau have been described, particularly for mid elevation ponderosa pine forests and lower elevation piñon–juniper woodlands. An overview is presented in Wilcox and Breshears (1995). In ponderosa pine forests, surface runoff may comprise 3–11% of the annual water budget (Wilcox *et al*., 1997). During winter snowmelt, subsurface shallow water flow (or interflow) is a significant hydrological process that can comprise as much as 20% of the annual water budget (Wilcox *et al*., 1996, 1997; Newman *et al*., 1998; Wilcox and Breshears, 1998). Soil water dynamics reflect the two large seasonal inputs of precipitation and a period of high evapotranspiration following each (Brandes, 1998; Brandes and Wilcox, 2000), with soil evaporation extending to a depth of ~10 cm and downward flux of ~0·02 cm year^{-1} (Newman *et al*., 1997).

In piñon–juniper woodlands, runoff also occurs in response to both snowmelt and summer rain (Wilcox, 1994). Within these woodlands, the runoff is highly spatially heterogeneous, with much of the runoff generated within bare patches and being redistributed to grassy patches; the canopy patches of trees generate runoff only following large, protracted frontal storms (Reid *et al*., 1999). Consequently, runoff at the hillslope scale is greatly reduced compared with that observed at the smaller scale of vegetation patches (Wilcox *et al*., 1996; Davenport *et al*., 1998; Reid *et al*., 1999). Aspects of temporal and spatial variation in soil water, evaporation and transpiration are presented in Lane and Barnes (1987), Breshears *et al*. (1997, 1998), and Newman *et al*. (1997).

Fire history and the Cerro Grande fire

The historical impacts of fire have been well documented for the Pajarito Plateau (Foxx, 1984; Allen, 1989; Swetnam and Betancourt, 1990; Swetnam and Baisan, 1996; Touchan *et al*., 1996; Allen *et al*., 1998; Swetnam *et al*., 1999). Prior to the arrival of the railroad and subsequent large increases in grazing, there were low-intensity fires recurring frequently, on the order of every 3–15 years for many of the ponderosa pine sites. Subsequently, fire frequencies decreased, due to reduction of fine herbaceous fuels and later due to direct suppression of forest fires, and this change in fire frequency led to increasing densities of woody vegetation on the Pajarito Plateau. The high density of trees within stands across the plateau changed the nature of fires to high-intensity crown fires that result in extensive tree mortality. On the Pajarito Plateau there have been three large-scale wildfires within the last 25 years: the La Mesa fire in 1977 (Foxx, 1984), the Dome fire in 1996 [see Cannon and Reneau (2000) and references cited therein] and the Cerro Grande fire in 2000. Post-fire studies documenting amplified hydrologic response include: Purtyman and Adams (1980), White and Wells (1984), and White (1996) for the La Mesa fire; Cannon and Reneau (2000) for the Dome fire; and Cannon *et al*. (2001), Johansen *et al*. (2001), and McLin *et al*. (2001) for the Cerro Grande fire.

The Cerro Grande fire burned nearly 17 300 ha total (8850 ha on the Plateau). The most severely burned areas were in densely forested locales, which created hydrophobic soil conditions (where volatilized organic matter condensed within the top layer of soil to create a waxy, impermeable, water-repellent barrier) as determined by the water-drop penetration time test observed by the BAER team.

METHODS

We performed hydrologic simulations using the landscape-scale, fully distributed ecohydrological model SPLASH (Martens *et al*., manuscript in preparation). SPLASH (Figure 1) includes simulation of lateral flows of surface and groundwater, infiltration, simulation of evapotranspiration from a vegetation canopy, an energy balance approach for snowpack calculations, and a climate simulator. The model can be used to examine these processes over periods of minutes to years. The landscape is represented in SPLASH as square grid cells within which most properties are considered to be homogeneous. SPLASH requires parameterization with a digital elevation model (DEM), six soil physical parameters, and leaf area index (LAI), and is able to use elevation lapse functions for temperature and precipitation. Driving variables are temperatures (daily maximum, minimum) and precipitation (daily or sub-daily). Four important attributes of SPLASH are physical representation of surface water routing, topographic shading, surface/subsurface hydrological coupling, and physically and biologically based representation of evaporation and transpiration.

SPLASH simulates overland flow using Manning's equation for calculating discharge, and routes water in the direction of steepest descent (aspect) based on the DEM. In SPLASH, water ponded on the surface by any means (e.g. saturation excess, infiltration excess) is subject to flow. Overland flow in SPLASH can be considered gradually varying sheetflow: the energy source for flow (gravity) is consumed by friction. The slope of the water surface is used to calculate the gradient between any two cells (diffusive wave approximation). [Optionally, the slope of the water surface may be assumed parallel to the bed (DEM) surface (kinematic wave approximation).] This allows SPLASH to simulate backwater effects and ponding of water in topographic depressions that may then overflow. SPLASH does not explicitly incorporate channel flow: channel flow in SPLASH occurs only inasmuch that 'channels' are defined by the DEM. SPLASH calculates water flow into or out of a cell through the four faces of that cell: two in the x direction, and two in the y direction. Velocities and discharges are calculated separately for each direction. For example, in the x direction:

$$u = \frac{1}{n} h_s^{2/3} S_x^{1/2}$$

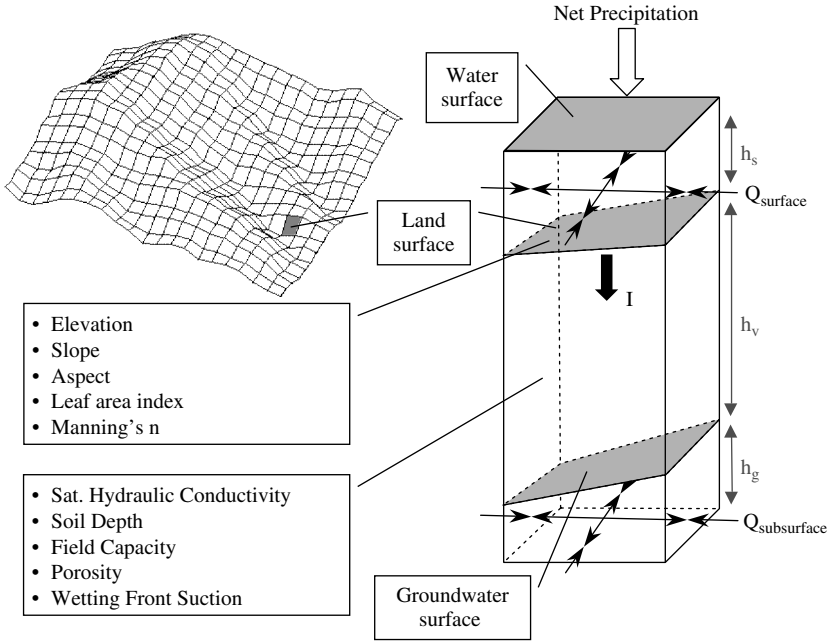

Figure 1. Hydrologic flows evaluated in the SPLASH model

where u is the velocity (m s^{-1}), n is Manning's roughness coefficient, h_s is the hydraulic radius [m, which reduces to flow depth (surface head) for overland flow], and S_x is the slope of surface head in the x direction (m m^{-1}). Discharge, Q (m^3 s^{-1}) is calculated as the product of velocity and cross-sectional area ($h_s \times$ cell size).

SPLASH uses an explicit, finite-difference calculation scheme, which allows algorithm simplicity. Time-step size Δt is dynamically determined by SPLASH based on a user-defined Courant number c (where $0 < c \leq 1$; Courant *et al.*, 1928), the cell size x, and the maximum flow velocity on the grid at the previous time step v_{max}:

$$\Delta t = c(x/v_{max})$$

Thus, if the maximum velocity is very large, the time step must be correspondingly small. Because SPLASH has a minimum time step size of 1 s, high flow velocities, which might occur in high-order channels, may cause numerical instability. A stream grid mask can be used by SPLASH to circumvent this possibility (by setting h_s to zero in each stream grid cell at each time step) at the cost of having no simulation of 'channel' flows in those cells.

SPLASH requires spatial inputs (maps) for parameters that describe topography, vegetation, and soil. We assembled these inputs using a geographic information system (ArcInfo, ArcView) from the best available sources.

Topography was represented using a DEM of 30 m × 30 m cells resampled from a ~5 m × ~5 m DEM obtained through a database maintained by Los Alamos National Laboratory. The rectangular area simulated was 898 by 756 cells (678 888 cells) and covered approximately 61 100 ha. The elevation range of the area simulated was from 1600 to 3200 m AMSL. We generated slope and aspect maps from this DEM using the methods in ArcInfo (ESRI, Redlands, CA). The average slope for the area simulated was 13·9°, and ranged from 0 to 69·4°. From the 30 m DEM, we generated a 'stream grid' using ArcInfo-calculated flow direction and flow accumulation grids. We set a threshold flow accumulation value of 200 cells, so that cells above this threshold of potential contributing area were considered 'stream' cells. We also prepared a basin mask grid that defined our area of interest within the rectangular area simulated, and masked from computation those areas that drained outside of the area of interest.

Vegetation types were derived from a summary of nine land-type classifications for the Pajarito Plateau (aspen forest 2%, bare ground 6%, developed 6%, grassland 4%, juniper woodland 3%, mixed conifer forest 23%, piñon/juniper woodland 30%, ponderosa pine forest 25%, water/shadows <1%). We assigned an LAI of 3·0 to aspen forest, 0·0 to bare ground and developed areas, 0·5 to grassland, 1·5 to juniper woodland, 5·0 to mixed conifer forest, 2·5 to piñon/juniper woodland, 3·5 to ponderosa pine forest, 2·0 to water/shadows. For the simulations presented here, LAI primarily influences canopy interception of precipitation. We also used vegetation type information for parameterizing the soil roughness descriptor, Manning's n. Based on the resistance factors for overland flow presented by HEC-1 (HEC, 1998; Table 3.5), we assigned bare ground and developed $n = 0{\cdot}02$, grassland $n = 0{\cdot}15$, juniper woodland $n = 0{\cdot}2$, piñon/juniper woodland $n = 0{\cdot}3$, ponderosa pine forest $n = 0{\cdot}4$, aspen and mixed conifer forest $n = 0{\cdot}5$, and water/shadows $n = 0{\cdot}3$.

A soil type map was constructed from three different sources in order to provide the best coverage of the area simulated on the plateau (Nyhan *et al.*, 1978; Benally, 1991; USDA, 1994). These sources varied in spatial resolution and degree of characterization of the soils. We used the surface (mineral) horizon description for characterizing the uniform soil profile required by SPLASH. For each soil type, we tabulated percent sand, percent clay, soil depth, and percent coarse fragments (>2 mm), which were used to calculate the soil hydraulic parameters for each soil type.

The soil hydraulic parameters required by SPLASH are porosity, field capacity, saturated hydraulic conductivity, and suction at the wetting front (for Green–Ampt infiltration). Porosity ϕ was calculated from bulk density BD and particle density PD using the relationship:

$$\phi = 1 - (BD/PD)$$

where PD = 2·65 g cm^{-3}. BD was calculated as a function of percent sand and percent clay using the equation of Rawls *et al*. (1992; Eqn 5.5.13), where organic matter and CEC/clay ratio were fixed at 0·5. Calculated ϕ was multiplied by a coarse fragment correction (CFC) factor (Brakensiek *et al*., 1986):

$$\text{CFC} = 1 - (\%\ \text{volume of coarse fragments}/100)$$

Field capacity was calculated from percent sand and percent clay using the equation of Saxton *et al*. (1986, Eqn 2). Saturated hydraulic conductivity K_s was calculated using the approach of Rawls and Brakensiek (1983; Eqn 8), where K_s is a function of porosity and the Brooks–Corey parameters: pore-size distribution index λ, bubbling pressure h_b, and residual water content θ_r (Brooks and Corey, 1964). K_s was multiplied by CFC to correct for coarse fragments. Suction at the wetting front S_f was calculated from porosity, percent sand, and percent clay using the equation of Rawls and Brakensiek (1985).

We conducted simulations for pre- and post-fire conditions using a low- and high-magnitude rain event. For the simulated rain events, we used 2 year (total 3·4 cm) or 100 year (total 6·63 cm) design storms (McLin, 1992), which have a peak intensity at mid-event (Figure 2). All simulations were conducted for 24 h following the initiation of the event. For post-fire simulations we modified the spatial distribution of SPLASH input parameters (LAI, K_s, and Manning's n) based on a burn severity map produced by the BAER team (Figure 3). The burn severity map classified burned areas as high (very little tree canopy remaining, and no ground cover remaining), moderate (some tree canopy remaining, but no ground cover remaining), or low severity (little to no fire occurred). The Cerro Grande fire affected about 30% of the area simulated, and of this area 53% was classified as high burn severity. We modified the LAI so that in high burn severity areas the LAI was reduced to 0·0, but it was left unchanged in other areas. Manning's n was assigned a value of 0·02 in high- and moderate-severity burn areas (including hydrophobic areas), where there was little ground cover remaining, but was left unmodified in low-severity areas, where little or no fire occurred. K_s was reduced to 0·0 on north-facing high-severity areas, where fire residence times are generally longer, to simulate a hydrophobic surface layer, in concurrence with the BAER report. For all simulations, vadose zone water content was initialized at 50% of field capacity, and surface water was set to zero. We used the stream grid (defined above) to mask these cells from computation by SPLASH. We set SPLASH to write surface discharge Q (m^3 s^{-1}) and surface head (h_s/m) at 2 min intervals of simulation time, which produced 720 maps of Q and h_s over the 24 h simulation period. For each of the four simulations, we then processed the output files from SPLASH to produce a map of the maximum Q for each cell during the 24 h simulation period.

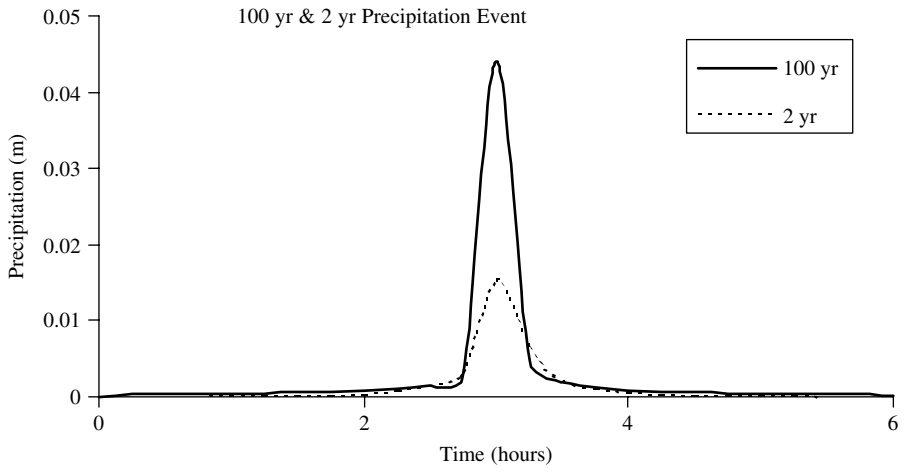

Figure 2. Hyetographs for 2 year and 100 year design storms

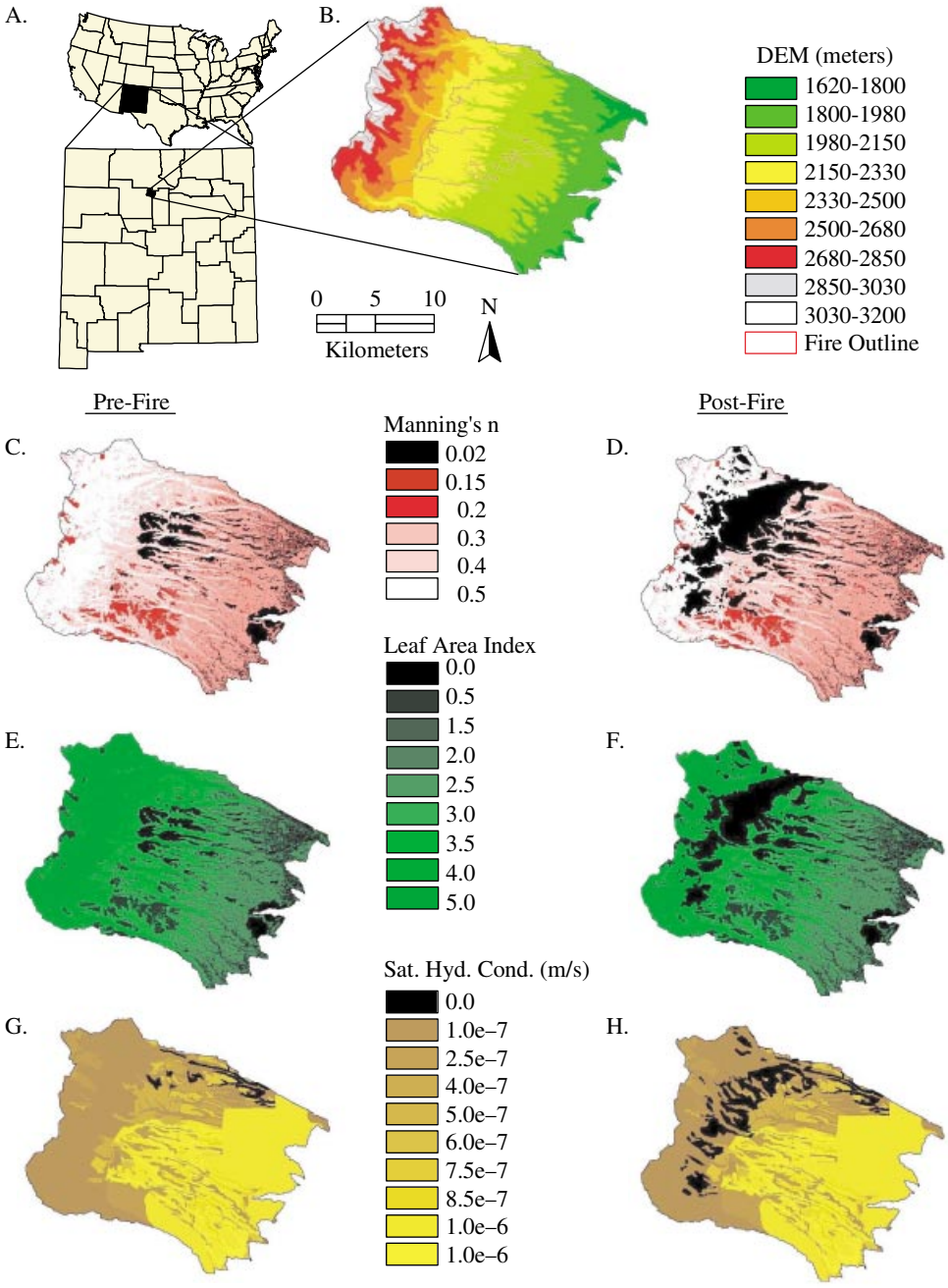

Figure 3. SPLASH model inputs. (A) Location map of the Pajarito Plateau within New Mexico. (B) DEM of the simulated area, used to create slope and aspect grids. The outlined area is the burned area, as defined by high- and moderate-severity burn. (C) Pre-fire Manning's roughness coefficient. (D) Post-fire Manning's roughness coefficient, where high and moderate burn areas were changed to $n = 0{\cdot}02$. (E) Pre-fire LAI. (F) Post-fire LAI, where high burn areas were changed to LAI $= 0{\cdot}0$. (G) Pre-fire saturated hydraulic conductivity. (H) Post-fire saturated hydraulic conductivity, where hydrophobic areas were changed to $K_s = 0{\cdot}0$ m s^{-1}

A preliminary model comparison indicated that SPLASH predictions are reasonable for assessing spatially distributed differences in runoff (Martens, Wilson, Beeson, and Breshears, unpublished data). Testing of spatially distributed models such as SPLASH is particularly challenging and is greatly limited by data availability. To test for reasonableness of predictions from SPLASH, we conducted a model comparison of SPLASH estimates of runoff with those obtained from the curve number method, as used by the BAER team. Our comparisons were for the 100 year post-fire simulation for areas affected by the fire. We made comparisons at the scale of subcatchments ($n = 548$), for which curve number estimates were obtained. The subcatchments encompassed areas much larger than the 30 m × 30 m cell size used for SPLASH. Consequently, the runoff predicted by SPLASH was totalled for each subcatchment and divided by subcatchment area. SPLASH predictions of runoff were significantly correlated to those from the curve number method at the subcatchment scale, yielding a correlation of $r = 0{\cdot}56$ ($P < 0{\cdot}01$). This comparison confirms that SPLASH is useful and appropriate for addressing our objectives of assessing spatially distributed runoff.

RESULTS

Hydrologic responses varied spatially and were significantly modified by the effects of fire (Figure 4). For the 2 year event the maximum Q map for the pre-fire simulation largely reflects topographic variability (Figure 4A), whereas in the post-fire simulation the maximum Q map is clearly affected by the burned area (Figure 4B). There were substantial increases in maximum Q over the burned area, by more than 500% in some areas (Figure 4C).

In the pre-fire scenario for the 100 year event there were much greater values of maximum Q than for the 2 year event (Figure 4D). In the post-fire scenario there were substantial increases in maximum Q in the burned area (Figure 4E), even though Q values were much higher overall in the pre-fire scenario. These increases can be seen in the percent increase map (Figure 4F), although they are not as extensive as those observed for the 2 year event. The already high values of Q in the 100 year scenario did not yield as great a percentage post-fire increase in Q as that seen for the 2 year event.

We summarized the spatial differences in terms of frequency distributions. For the burned area, the frequency distribution of maximum Q across cells shifted notably from the pre-fire to the post-fire simulations for both event types (Figure 5). This shift occurred in terms of both an increase in modal value and a reduction in variance: 2 year pre-fire mode of $3{\cdot}25 \times 10^{-10}$ m^3 s^{-1} versus 2 year post-fire mode of $7{\cdot}0 \times 10^{-10}$ m^3 s^{-1}; 100 year pre-fire mode of $31{\cdot}8 \times 10^{-10}$ m^3 s^{-1} versus 100 year post-fire mode of $48{\cdot}6 \times 10^{-10}$ m^3 s^{-1}. Outside the burned area there were many locations where the post-fire runoff increased in our simulations, which account for the redistribution of water across cells. For the 2 year event, outside the burned area there were 5736 cells (30 m × 30 m each) that increased by more than 200% and 2515 cells that increased by more than 500%; similarly, for the 100 year event, there were 4447 cells that increased by more than 200% and 1598 cells that increased by more than 500%.

The effects of topography and surface conditions, as modified by the fire, are evident in the responses of individual locations within the plateau. We contrasted two locations within the burned area—a mesa top cell and a hillside cell (Figure 6A). These locations differ particularly with respect to slope and K_s (Figure 6B). The differences in the response of Q between mesa top and hillside for the pre-fire simulation illustrate the much sharper hydrograph peak for the hillside (Figure 6C). In contrast, for the post-fire simulation the mesa top hydrograph becomes larger and more peaked, whereas there is little change in the hydrograph for the hillside location (Figure 6D). For h_s, under the pre-fire simulation, the mesa top value is much larger than the hillside value, indicating the potential for water to pond on the mesa top but not on the steeper hillside. For the post-fire simulation, h_s is reduced at the mesa top location, but still exceeds that of the hillside location, which is essentially the same for both pre- and post-fire simulations. These differences highlight the ability of the model to simulate the interactive effects of topography and surface properties.

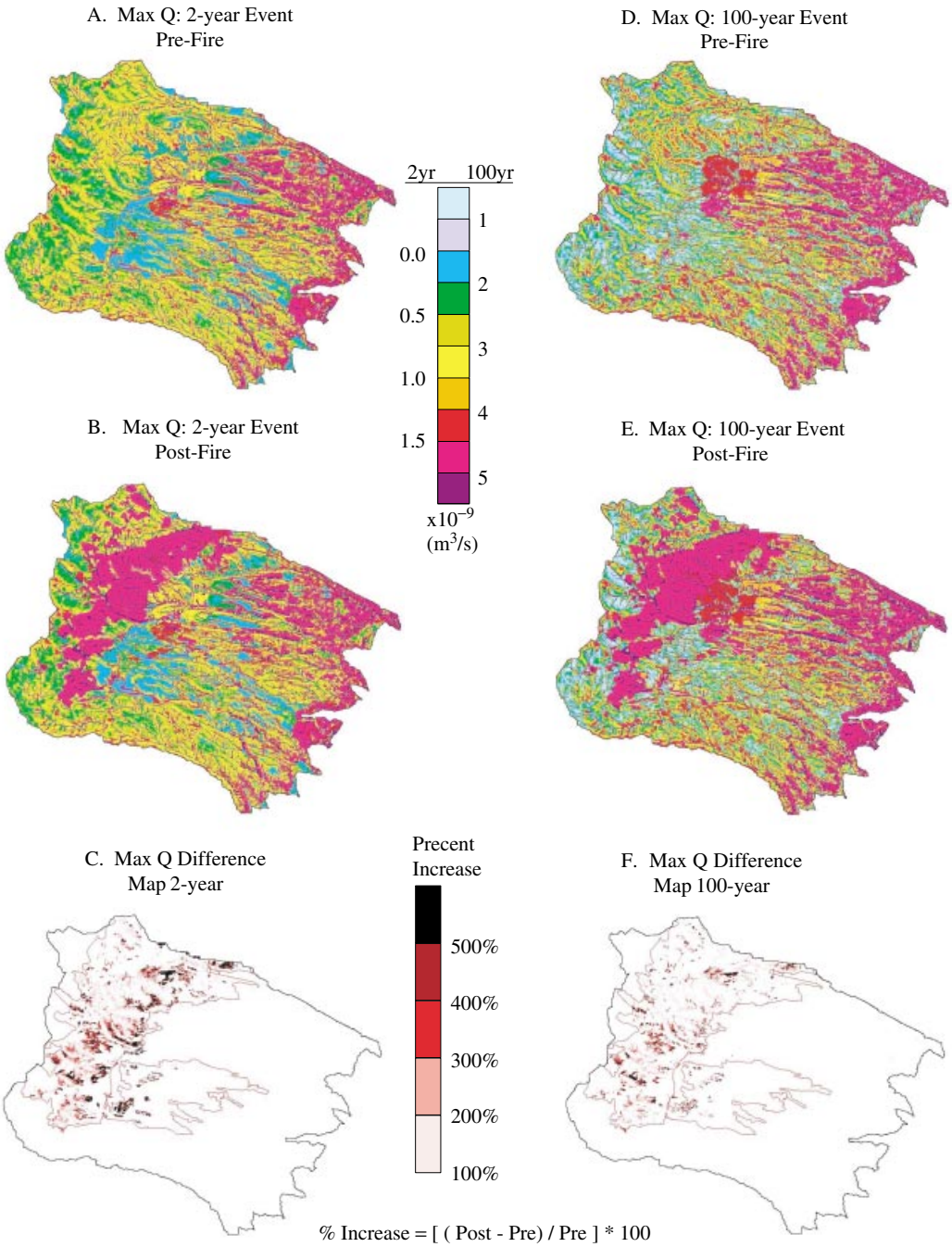

Figure 4. Simulation results for 2 year and 100 year precipitation events. (A) Maximum Q for the 2 year event, pre-fire simulation. (B) Maximum Q for the 2 year event, post-fire simulation. (C) Percent increase for the 2 year event simulations. (D) Maximum Q for the 100 year event, pre-fire simulation. (E) Maximum Q for the 100 year event, post-fire simulation. (F) Percent increase for the 100 year event simulations

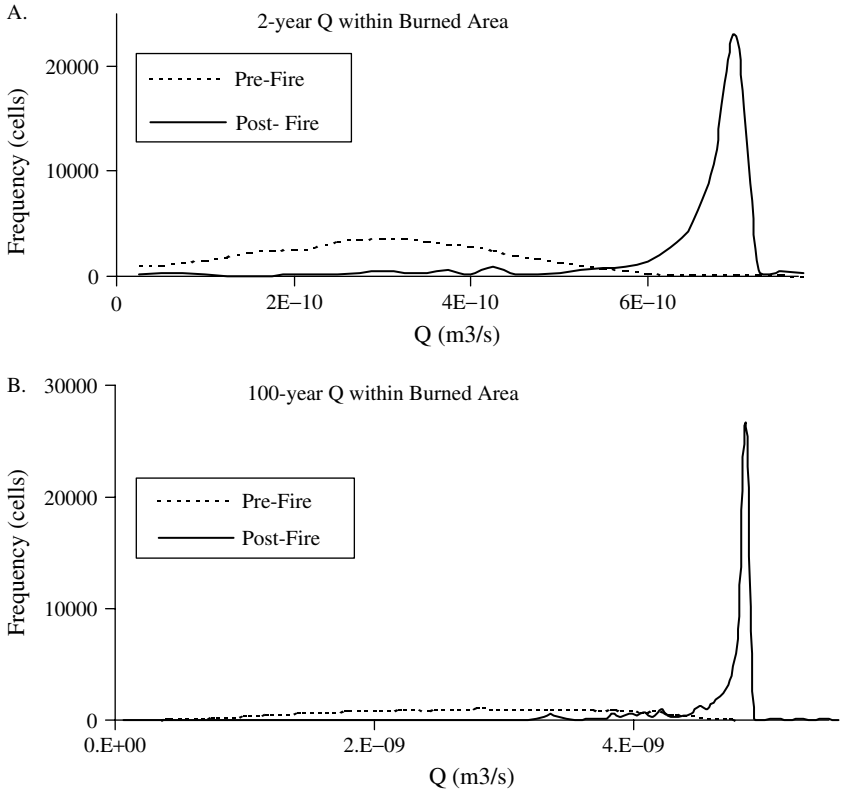

Figure 5. Frequency distributions of maximum Q within the burned area. (A) 2 year event, pre- and post-fire frequency distributions. (B) 100 year event, pre- and post-fire frequency distributions

DISCUSSION

Our model simulations highlight an approach that provides a spatially explicit assessment of post-disturbance impacts on overland flow—in this case impacts from severe wildfire. There were substantial increases in overland flow following fire for both the 2 year and the 100 year storm simulations (Figure 4). As expected, the greatest increase in overland flow occurred on high-severity burn locations, particularly those with steep slopes. The vulnerability indices, which quantify post-fire increases in peak runoff, demonstrate how runoff increases in response to fire-induced changes in surface properties and how that impact depends on event size. Not surprisingly, our results suggest that there are likely to be substantial post-fire increases of runoff in channels.

The spatially distributed approach highlighted here represents an important advance in post-fire hydrological assessment. Most management remediation activities cannot focus at the broad scale of watersheds, but rather must focus on a subset of smaller areas that correspond much more closely to the 30 m × 30 m cell size used in these simulations. Hence, information is needed at a scale finer than watersheds. Further, although other methods may allow evaluation of a few to tens of *a priori* selected locations, our approach allows evaluation of thousands of locations (more than 670 000 30 m × 30 m cells in this example). In addition, the modelling approach presented here considers hydrological connectivity directly. We identified more than 5500 cells for which post-fire runoff outside the burned area increased more than 200% following the 2 year event; similarly, we identified more than 4000 cells for which post-fire runoff increased by more than 200% following the 100 year event. Other approaches would likely average across larger areas, thereby diluting the effects of these cells, or would only evaluate a very small subset of them. Our results highlight the importance of

A.

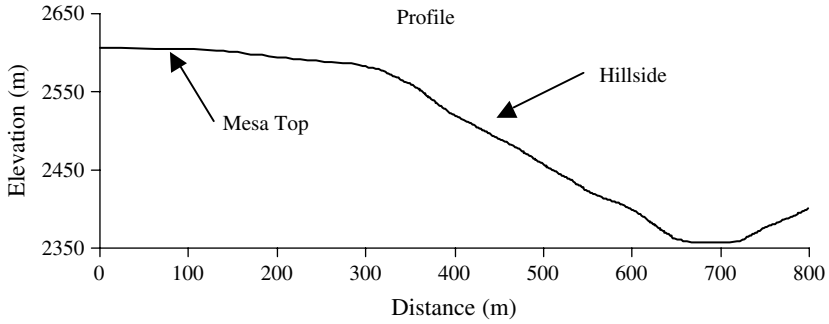

B.

	LAI	Mn	Ks	Slope (d)	Aspect	Elevation (m)
Pre - Mesa Top	3.5	0.4	9.1e-7	5.7	71.22	2603.3
Post - Mesa Top	0.0	0.02	0.0			
Pre - Hillside	5.0	0.5	3.8e-7	39.6	20.47	2549.1
Post - Hillside	0.0	0.02	0.0			

C.

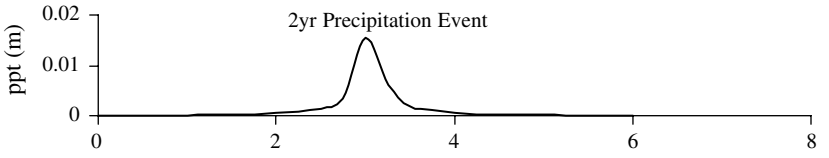

D.

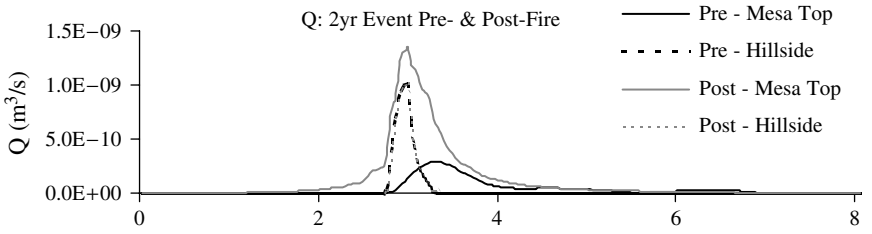

E.

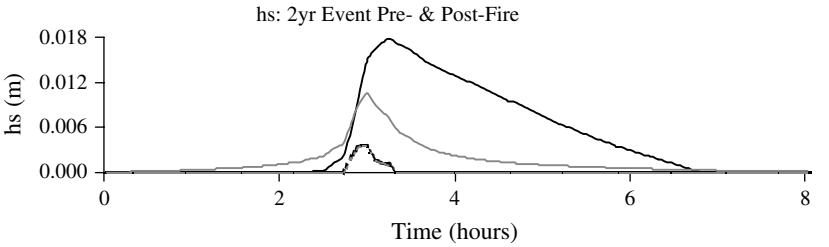

Figure 6. Contrast of mesa top and hillside locations for the 2 year event, pre- and post-fire. (A) Elevational cross-section. (B) Parameters used in simulations. (C) 2 year event hyetograph. (D) 2 year event hydrograph of Q (m^3 s^{-1}). (E) 2 year event surface head (m) hydrograph

explicitly evaluating hydrological connectivity among landscape spatial units in assessing post-fire response. More specifically, the difference maps presented in Figure 4C and F represent not only the effects of changes in surface properties, but also the effects of water that has been redistributed to a given cell from adjacent cells. Our simulations suggest that hydrological connectivity increases substantially following fire and identify those areas where this is so.

The ability to map quantitatively and identify areas vulnerable to increased runoff, as presented here, provides an important means for comprehensively assessing post-fire response over a large region. These maps could be useful tools for managers in the future. This type of information can be used to prioritize post-fire remediation activities (e.g. McLin *et al*., 2001; Wilson *et al*., 2001). The development and deployment of this approach as a tool depends on advanced planning that includes development of soils and vegetation maps, consideration of appropriate hydrologically relevant parameters, and access to adequate computing power.

Our results showing large increases in runoff are consistent with rainfall simulation studies at the site. Within ponderosa pine, runoff increased greatly following the Cerro Grande fire (Johansen *et al*., 2001). Similarly, runoff in piñon–juniper woodlands increased greatly following other types of disturbance, such as manual removal of herbaceous plants (Wilcox, 1994). The frequency and intensity of disturbance events such as fire are expected to increase in the future (Lenihan *et al*., 1998; Swetnam *et al*., 1999; Easterling *et al*., 2000). Hence, it will be increasingly important to be able to assess rapidly and effectively post-fire changes in hydrology and to apply these assessments to evaluate risks to infrastructure. Our approach for assessing spatially distributed runoff could be coupled with other essential components of post-fire assessment, such as sediment yields (Wilson *et al*., 2001) and channel flows (McLin *et al*., 2001). The modelling approach demonstrated here using SPLASH indicates the possibilities and potential benefits of adopting such an approach. More generally, our study highlights the large and spatially explicit nature of the effects of fire on landscape-scale hydrology and provides an approach for prioritizing post-fire remediation activities.

ACKNOWLEDGEMENTS

This work was funded by Los Alamos National Laboratory: initial funding was provided by Post-Fire Emergency Response; additional work was supported by the Institute for Geophysics and Planetary Physics for Los Alamos/University of California Davis collaboration; training on SPLASH for PCB was provided through the Undergraduate Research Semester. We wish to thank the following for their support, assistance, and comments: C. J. Wilson, S. L. Ustin, the Ecology Group (ESH-20) for providing vegetation data, and SUN Computers for loan of an Ultra80 in the weeks following the Cerro Grande fire.

REFERENCES

Allen CD. 1989. *Changes in the landscape of the Jemez Mountains, New Mexico*. PhD Dissertation, University of California Berkley.

Allen CD, Breshears DD. 1998. Drought-induced shift of a forest–woodland ecotone: rapid landscape response to climate variation. *Proceedings of the National Academy of Sciences USA* **95**: 14 839–14 842.

Allen CD, Betancourt JL, Swetnam TW. 1998. Landscape changes in the southwestern United States: techniques, long-term data sets, and trends. In *Perspectives on the land-use history of North America: a context for understanding the changing environment*, Sisk TD (ed). US Geological Survey, Biological Resources Division, Biological Science Report USGS/BRD/BSR-1998-0003; 71–84.

Barnes FJ. 1986. *Carbon gain and water relations in pinyon–juniper habitat types*. PhD Dissertation. New Mexico State University, Las Cruces, NM.

Benally Jr EK. 1991. *Terrestrial ecosystem survey of the Santa Fe National Forest*. United States Department of Agriculture, Forest Service, Southwestern Region.

Bowen BM. 1990. *Los Alamos climatology*. Los Alamos National Laboratory Report LA-11735-MS.

Brakensiek DL, Rawls WJ, Stephenson GR. 1986. A note on determining soil properties for soils containing rock fragments. *Journal of Range Management* **39**: 408–409.

Brandes D. 1998. *A low-dimensional dynamical model of hillslope soil moisture with application to a semiarid field site*. PhD Dissertation. The Pennsylvania State University. (Also Los Alamos National Laboratory Report LAUR-98-4228.)

Brandes D, Wilcox BP. 2000. Evapotranspiration and soil moisture dynamics on a semiarid ponderosa pine hillslope. *Journal of the American Water Resources Association* **36**: 965–974.

Breshears DD, Rich PM, Barnes FJ, Campbell K. 1997. Overstory-imposed heterogeneity in solar radiation and soil moisture in a semiarid woodland. *Ecological Applications* **7**: 1201–1215.

Breshears DD, Nyhan JW, Heil CE, Wilcox BP. 1998. Effects of woody plants on microclimate in a semiarid woodland: soil temperature and evaporation in canopy and intercanopy patches. *International Journal of Plant Sciences* **159**: 1010–1017.

Brooks RH, Corey AT. 1964. *Hydraulic properties of porous media*. Hydrology Paper No. 3, Colorado State University, Fort Collins.

Cannon SH, Reneau SL. 2000. Conditions for generation of fire-related debris flows, Capulin Canyon, New Mexico. *Earth Surface Processes and Landforms* **25**: 1103–1121.

Cannon SH, Powers PS, Savage WZ. 1998. Fire-related hyperconcentrated and debris flows on Storm King Mountain, Glenwood Spring, Colorado. U.S.A. *Environmental Geology* **35**: 210–217.
Cannon SH, Bigio ER, Mine E. 2001. A process for fire-related debris-flow initiation, Cerro Grande fire New Mexico. *Hydrological Processes* **15**: 3011–3023.
Courant R, Friedrichs KO, Lewy H. 1928. Uber die partiellen differenzengleichngen der mathematishen physik. *Mathematische Annalen* **100**: 32–74.
Covington WW, Everett RL, Steele R, Irwin LL, Daer TA, Auclaire AND. 1994. Historical and anticipated changes in forest ecosystems in the inland west of the United States. *Journal of Sustainable Forestry* **2**: 13–63.
Davenport DW, Wilcox BP, Breshears DD. 1996. Soil morphology of canopy and intercanopy sites in a piñon–juniper woodland. *Soil Science Society of America Journal* **60**: 1881–1887.
Davenport DW, Breshears DD, Wilcox BP, Allen CD. 1998. Viewpoint: sustainability of piñon–juniper ecosystems: a unifying perspective of soil erosion thresholds. *Journal of Range Management* **51**: 231–240.
DeBano LF. 2000. Water repellency in soils: a historical overview. *Journal of Hydrology* **231–232**: 4–32.
Dietrich WE, Wilson CJ, Montgomery DR, McKean J. 1993. Analysis of erosion thresholds, channel networks, and landscape morphology using a digital terrain model. *Journal of Geology* **101**: 259–278.
Easterling DR, Meehl GA, Parmesan C, Changnon SA, Karl TA, Mearns LO. 2000. Climate extremes: observations, modeling, and impacts. *Science* **289**: 2068–2074.
Foxx TS. (compiler). 1984. *La Mesa Fire Symposium*, Los Alamos New Mexico, October 6–7, 1981. Los Alamos National Laboratory Report LA-9236-NERP.
HEC. 1998. *HEC-1 Flood Hydrograph Package Users Manual, CPD-1A*. US Army Corps of Engineers, Hydrologic Engineering Center, Davis, CA.
Herbel CH, Ares FN, Wright RA. 1972. Drought effects on a semidesert grassland range. *Ecology* **53**: 1084–1093.
Herron N, Wilson C. 2001. A water balance approach to assessing the hydrologic buffering potential of an alluvial fan. *Water Resources Research* **37**: 341–351.
Johansen M, Hakonson TE, Breshears DD. 2001. Post-fire runoff and erosion from rainfall simulation: contrasting forests with shrublands and grasslands. *Hydrological Processes* **15**: 2953–2965.
Lane LJ, Barnes FJ. 1987. Water balance calculations in Southwestern woodlands. In *Proceedings, Pinyon–Juniper Conference*. USDA Forest Service Intermountain Research Station General Technical Report INT-215. USDA Forest Service, Fort Collins, CO; 480–488.
Lenihan JM, Daly C, Bachelet D, Neilson RP. 1998. Simulating broad-scale fire severity in a dynamic global vegetation model. *Northwest Science* **72**: 91–103.
Martens SN, Breshears DD, Barnes FJ. 2001. Development of species dominance along an elevational gradient: population dynamics of Pinus edulis and Juniperus monosperma. *International Journal of Plant Sciences* **162**: 777–783.
Martens SN, Ustin SL, Wallender WW. SPLASH: A simulator for processes of landscapes: surface/subsurface hydrology. In preparation
Mast JN, Fulé PZ, Moore MM, Covington WW, Waltz AEM. 1999. Restoration of presettlement age structure of an Arizona ponderosa pine forest. *Ecological Applications* **9**: 228–239.
McLin SG. 1992. *Determination of 100-year floodplain elevations at Los Alamos National Laboratory*. LA-12195.
McLin SG, Springer EP, Lane LJ. 2001. Predicting floodplain boundary changes following the Cerro Grande wildfire. *Hydrological Processes* **15**: 2967–2980.
Meyer GA, Wells SG. 1997. Fire-related sedimentation events on alluvial fans, Yellowstone National Park, U.S.A. *Journal of Sedimentary Research* **67**: 776–791.
Moore MM, Covington WW, Fulé PZ. 1999. Reference conditions and ecological restoration: a Southwestern pondereosa pine perspective. *Ecological Applications* **9**: 1266–1277.
Morris SE, Moses TA. 1987. Forest-fire and natural soil erosion regime in the Colorado Front Range. *Annals of the Association of American Geographer* **77**: 245–254.
Newman BD, Campbell AR, Wilcox BP. 1997. Tracer-based studies of soil water movement in semi-arid forest of New Mexico. *Journal of Hydrology* **196**: 251–270.
Newman BD, Campbell AR, Wilcox BP. 1998. Lateral subsurface flow pathways in a semiarid ponderosa pine hillslope. *Water Resources Research* **34**: 3485–3496.
Nyhan JW, Hacker LW, Calhoun TE, Young DL. 1978. *Soil survey of Los Alamos County, New Mexico*. Los Alamos National Laboratory Report LA-6779-MS.
Padien DJ, Lajtha K. 1992. Plant spatial pattern and nutrient distribution in pinyon–juniper woodlands along an elevational gradient in northern New Mexico. *International Journal of Plant Sciences* **153**: 425–433.
Prosser IP, Williams L. 1998. The effect of wildfire on runoff and erosion in a native Eucalyptus forest. *Hydrological Processes* **12**: 251–265.
Purtyman WD, Adams H. 1980. Geohydrology of Bandelier National Monument, New Mexico. Los Alamos National Laboratory Report LA-8461-MS.
Rawls WJ, Brakensiek DL. 1983. A procedure to predict Green Ampt infiltration parameters. In *Advances in Infiltration: Proceedings of the National Conference on Advances in Infiltration*. ASAE publication, 83-11. American Society of Agricultural Engineers: St Joseph, MI; 102–112.
Rawls WJ, Brakensiek DL. 1985. Prediction of soil water properties for hydrologic modeling. In *Watershed Management in the Eighties: Proceedings of the Symposium*. American Society of Civil Engineers: New York, NY; 293–299.
Rawls WJ, Ahuja LR, Brakensiek DL, Shirmohammadi A. 1992. Infiltration and soil water movement. In *Handbook of Hydrology*, Maidment DR (ed.). McGraw-Hill: New York; Chapter 5.
Regensberg A. 1996. General dynamics of drought, ranching, and politics in New Mexico, 1953–1961. *New Mexico Historical Review* **71**: 25–49.

Reid KD, Wilcox BP, Breshears DD, MacDonald L. 1999. Runoff and erosion in a piñon–juniper woodland: influence of vegetation patches. *Soil Science Society of America Journal* **63**: 1869–1879.
Robichaud PR, Beyers JL, Neary DG. 2000. *Evaluating the effectiveness of postfire rehabilitation treatments*. USDA Forest Service Rocky Mountain Station General Technical Report RMRS-GTR-63. USDA Forest Service, Fort Collins, CO.
Saxton KE, Rawls WJ, Romberger JS, Papendick RI. 1986. Estimating generalized soil-water characteristics from texture. *Soil Science Society of America Journal* **50**: 1031–1036.
Seyfried MS, Wilcox BP. 1995. Scale and the nature of spatial variability: field examples having implications for hydrological modeling. *Water Resources Research* **31**: 173–184.
Swetnam TW, Betancourt JL. 1990. Fire–Southern Oscillation relations in the southwestern United States. *Science* **249**: 1017–1020.
Swetnam TW, Baisan CH. 1996. Historical fire regime patterns in the southwestern United States since AD 1700. In *Fire Effects in Southwestern Forests. Proceedings of the Second La Mesa Fire Symposium*, Allen CD (ed.). USDA Forest Service General Technical Report RM-GTR-286; 11–32.
Swetnam TW, Betancourt JL. 1998. Mesoscale disturbance and ecological response to decadal climatic variability in the American Southwest. *Journal of Climate* **11**: 3128–3147.
Swetnam TW, Allen CD, Betancourt JL. 1999. Applied historical ecology: using the past to manage the future. *Ecological Applications* **9**: 1189–1206.
Touchan R, Allen CD, Swetnam TW. 1996. Fire history and climatic patterns in ponderosa pine and mixed-conifer forests of the Jemez Mountains, northern New Mexico. In *Fire Effects in Southwestern Forests. Proceedings of the Second La Mesa Fire Symposium*, Allen CD (ed.). USDA Forest Service General Technical Report RM-GTR-286; 33–46.
US Department of Agriculture, Soil Conservation Service. 1994. *State Soil Geographic (STATSGO) Database for New Mexico*. USDA: Fort Worth, TX.
White WD. 1996. Geomorphic response to six headwater basins fifteen years after the La Mesa Fire. In *Fire Effects in Southwestern Forests. Proceedings of the Second La Mesa Fire Symposium*, Allen CD (ed.). USDA Forest Service General Technical Report RM-GTR-286; 95–113.
White WD, Wells SG. 1984. Geomorphic effects of La Mesa Fire. In *La Mesa Fire Symposium*, Foxx TS (compiler). LA_9236-NERP; 73–90.
Wilcox BP. 1994. Runoff and erosion in intercanopy zones of pinyon–juniper woodlands. *Journal of Range Management* **47**: 285–295.
Wilcox BP, Breshears DD. 1995. Hydrology and ecology of piñon–juniper woodlands: conceptual framework and field studies. In *Desired Future Conditions for Piñon–Juniper ecosystems*, Shaw DW, Aldon EF, LoSapio C (coordinators). USDA Forest Service General Technical Report RM-258. Fort Collins, CO; 109–119.
Wilcox BP, Breshears DD. 1998. Interflow in a semiarid environments: an overlooked process in risk assessment. *Human and Ecological Risk Assessment* **3**: 187–203.
Wilcox BP, Newman BD, Allen CD, Reid KD, Brandes D, Pitlick J, Davenport DW. 1996. Runoff and erosion on the Pajarito Plateau: observations from the field. In *New Mexico Geological Society Guidebook*, Goff F *et al*. (eds). New Mexico Geological Society: Socorro, NM; 433–439.
Wilcox BP, Newman BD, Brandes D, Davenport DW, Reid K. 1997. Runoff from a semiarid ponderosa pine hillslope site in New Mexico. *Water Resources Research* **33**: 2301–2314.
Wilson CJ. 1999. Effects of logging and fire on runoff and erosion on highly erodible granitic soils in Tasmania. *Water Resources Research* **35**: 3531–3546.
Wilson CJ, Carey JW, Beeson PC, Gard MO, Lane LJ. 2001. A GIS-based hillslope erosion and sediment delivery model and its application in the Cerro Grande burn area. *Hydrological Processes* **15**: 2995–3010.

